



Role and modelling of some heterogeneities for cardiac electrophysiology

Andjela Davidović,
INRIA, University of Bordeaux, IMB, Lyric

Contents

Modelling

Multiscale models

The cellular level

The tissue level

The bidomain model

The tissue heterogeneities

The new model

Mesoscale model

Homogenisation

Two-scale convergence method

Macroscale model

Numerics

Convergence

Homogenisation

Comparison

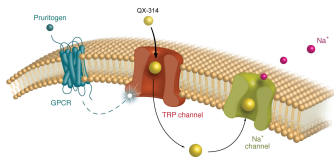
1

The first chapter

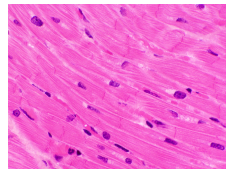
Modelling

Multiscale models

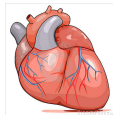
Cellular level



Tissue level

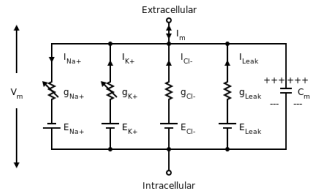
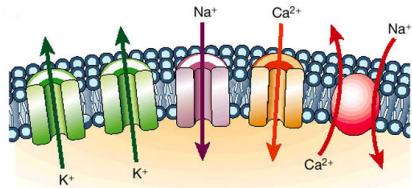


Organ level



Larger scale models depend on the smaller scale model.

The cellular level



- ▶ Cardiomyocytes - excitable cells, action potential (AP)
- ▶ Modelling
 - ▶ membrane - capacitor
 - ▶ ionic channels - conductors
 - ▶ ionic pump - source

$$I = \frac{dv}{dt} + I_{ion}(v)$$

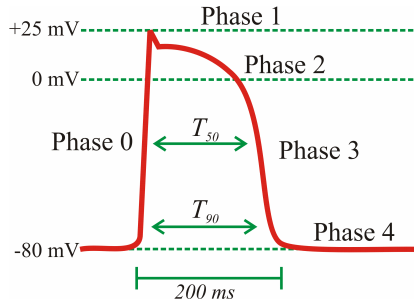
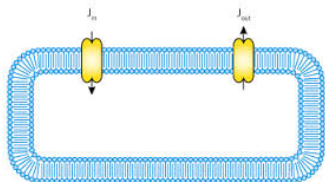
- ▶ I_{ion} - sum of ionic currents, ODEs
- ▶ Up to 15 different ionic currents

Mitchell-Schaeffer model

$$I_{ion}(v, h) = \frac{1}{\tau_{in}} hv^2(v - 1) - \frac{1}{\tau_{out}} v$$

$$\partial_t h + g(v, h) = 0$$

$$g(v, h) = \begin{cases} \frac{1-h}{\tau_{open}}, & \text{if } v < v_{gate}, \\ \frac{-h}{\tau_{close}}, & \text{if } v \geq v_{gate} \end{cases}$$



The tissue level

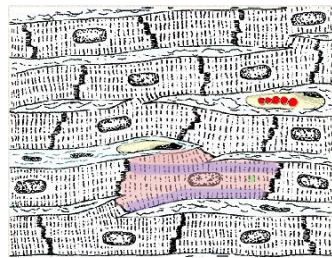
What do we model?

Propagation of AP

- ▶ Gap junctions
- ▶ Communication
- ▶ Coordinated contraction

Problem

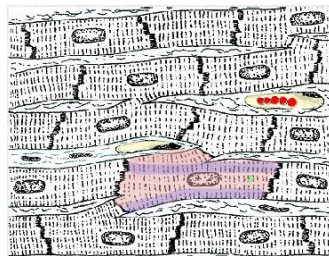
- ▶ Huge number of equations
- ▶ Huge number of transmission conditions
- ▶ Very small space step



The tissue level I

Mathematical assumptions:

- ▶ periodic micro-structure
- ▶ anisotropic intra- and extra-cellular spaces
- ▶ the transmembrane potential
- cable equation



Microscale model \rightarrow *homogenisation* \rightarrow **BIDOMAIN MODEL**

The bidomain model

Degenerate parabolic reaction-diffusion system + ODE

$$\begin{aligned}\partial_t v + I_{ion}(v, h) &= \nabla \cdot (\sigma_i \nabla u_i), && \text{in } \Omega, \\ \partial_t v + I_{ion}(v, h) &= -\nabla \cdot (\sigma_e \nabla u_e), && \text{in } \Omega, \\ \partial_t h + g(v, h) &= 0, && \text{in } \Omega.\end{aligned}$$

$v = u_i - u_e$ - transmembrane potential

The standard boundary conditions for isolated heart:

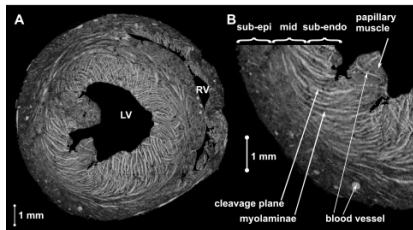
$$\begin{aligned}(\sigma_i \nabla u_i) \cdot n &= 0, \text{ on } \partial\Omega, \\ (\sigma_e \nabla u_e) \cdot n &= 0, \text{ on } \partial\Omega.\end{aligned}$$

The Gauge condition:

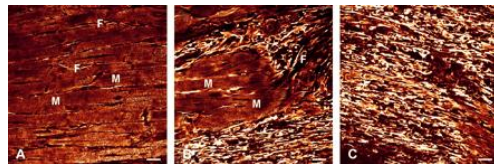
$$\int_{\Omega} u_e = 0.$$

Not a conclusive model - tissue heterogeneities

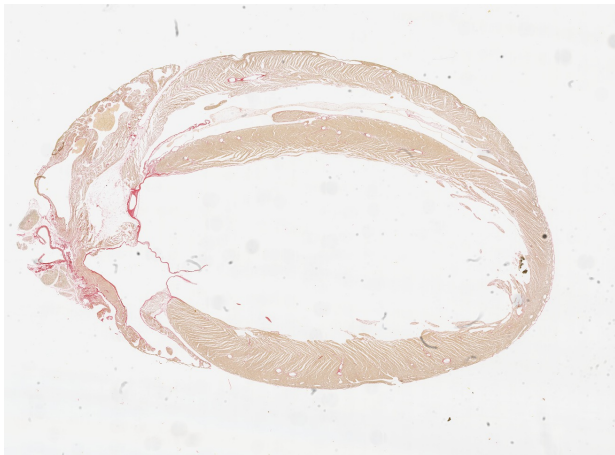
- ▶ Laminar stricture.



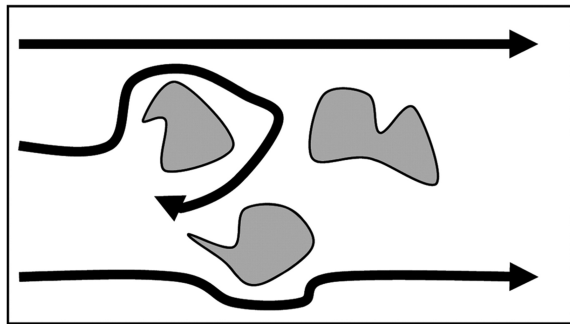
- ▶ The scar border zone.



Structural heterogeneities



Reentry



Long APD Region



Short APD Region

2

The second chapter

The new model

The new mesoscale model

Assumption: periodic diffusive inclusions

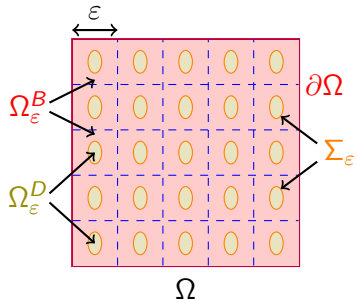


Figure: The 2D full domain Ω .

The new mesoscale model I

$$\left. \begin{array}{l} \partial_t v_\varepsilon + I_{ion}(v_\varepsilon, h_\varepsilon) = \nabla \cdot (\sigma^i \nabla u_\varepsilon^i), \\ \partial_t v_\varepsilon + I_{ion}(v_\varepsilon, h_\varepsilon) = \nabla \cdot (\sigma^e \nabla u_\varepsilon^e), \\ \partial_t h_\varepsilon + g(v_\varepsilon, h_\varepsilon) = 0. \end{array} \right\} \text{Bidomain}$$
$$0 = \nabla \cdot (\sigma^d \nabla u_\varepsilon^d), \quad \text{Diffusive incl.}$$

$v = u_i - u_e$ - transmembrane potential.

σ_i, σ_e - the standard anisotropic conductivities.

σ_d - the isotropic conductivity in the diffusive region.

$$\left. \begin{array}{l} (\sigma^i \nabla u_\varepsilon^i) \cdot n = 0, \\ (\sigma^e \nabla u_\varepsilon^e) \cdot n = (\sigma^d \nabla u_\varepsilon^d) \cdot n, \\ u_\varepsilon^e = u_\varepsilon^d. \end{array} \right\} \underline{\text{on the inner boundary ??}}$$

The new mesoscale model II

We write

$$u_\varepsilon = \begin{cases} u_\varepsilon^e, & \text{in } \Omega_\varepsilon^B, \\ u_\varepsilon^d, & \text{in } \Omega_\varepsilon^D, \end{cases} \quad \sigma = \begin{cases} \sigma_e, & \text{in } \Omega_\varepsilon^B, \\ \sigma_d, & \text{in } \Omega_\varepsilon^D. \end{cases}$$

The problem

$$\begin{aligned} \partial_t v_\varepsilon + I_{ion}(v_\varepsilon, h_\varepsilon) &= \nabla \cdot (\sigma^i \nabla u_\varepsilon^i), & \text{in } \Omega_\varepsilon^B, \\ \chi_{\Omega_\varepsilon^B}(\partial_t v_\varepsilon + I_{ion}(v_\varepsilon, h_\varepsilon)) &= \nabla \cdot (\sigma \nabla u_\varepsilon), & \text{in } \Omega, \\ \partial_t h_\varepsilon + g(v_\varepsilon, h_\varepsilon) &= 0, & \text{in } \Omega_\varepsilon^B. \end{aligned}$$

On the inner boundary

$$(\sigma^i \nabla u_\varepsilon^i) \cdot n = 0$$

Homogenisation

Main idea:

- Given model:

$$L_\varepsilon(u_\varepsilon) = f$$

- Assume: $u_\varepsilon \rightarrow u$

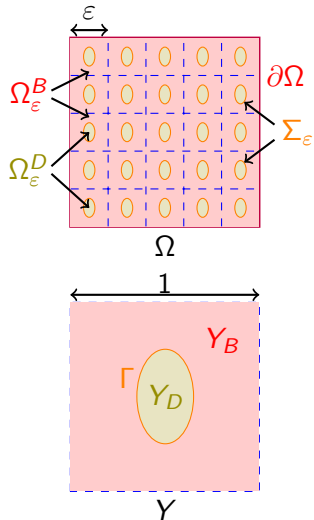
- Find L s.t.

$$L(u) = f$$

Formal approach

$$u_\varepsilon(x) = u_0(x) + \varepsilon u_1(x, x/\varepsilon) + \dots$$

$$u_1(x, y) = w(y) \cdot \nabla u_0(x)$$



Two-scale convergence method (Allaire)

- ▶ Rigorous, exploits periodicity
- ▶ Solves two problems simultaneously
- ▶ New convergence definition - specific periodic test functions
- ▶ Requires: uniform *a priori* estimates, independent of ε

Method

1. Existence of $(v_\varepsilon, u_\varepsilon^i, u_\varepsilon)$ for fixed ε (Boulakia et al.)
2. *A priori* bounds
 - ▶ energy estimates for $v_\varepsilon, h_\varepsilon, \nabla u_\varepsilon^i, \nabla u_\varepsilon^e$
 - ▶ bound on non-linear functions $I_{ion}(v, h)$ and $g(v, h)$

Method

3. Derivation of twoscale homogenisation system - var. form.

- ▶ From the bounds

$$v_\varepsilon \rightarrow v_0, \quad h_\varepsilon \rightarrow h_0$$

- ▶ Derived convergence

$$\nabla u_\varepsilon^i \rightarrow \nabla u_0^i(x) + \nabla_y u_1^i(x, y), \quad \nabla u_\varepsilon \rightarrow \nabla u_0(x) + \nabla_y u_1(x, y)$$

- ▶ assume I_{ion} - Lipschitz function!

$$I_{ion}(v_\varepsilon, h_\varepsilon) \rightarrow I_{ion}(v_0, h_0), \quad g(v_\varepsilon, h_\varepsilon) \rightarrow g(v_0, h_0)$$

4. Express $u_1^i = w_i \cdot \nabla u_0^i$ and $u_1 = w \cdot \nabla u_0$.
5. Read off the homogenised and the cell problems.

The new macroscale model

$$\begin{aligned}(\partial_t v_0 + I_{ion}(v_0, h_0)) &= \nabla \cdot (\sigma_i^* \nabla u_0^i), && \text{in } \Omega, \\(\partial_t v_0 + I_{ion}(v_0, h_0)) &= -\nabla \cdot ((\sigma_e^* + \sigma_d^*) \nabla u_0), && \text{in } \Omega, \\\partial_t h_0 + g(v_0, h_0) &= 0, && \text{in } \Omega.\end{aligned}$$

New effective conductivities

$$\sigma_{i_{kj}}^* = \sigma_{i_{kj}} + \frac{1}{|Y_B|} (\sigma_{i_{k1}} A_{1j}^i + \sigma_{i_{k2}} A_{2j}^i + \sigma_{i_{k3}} A_{3j}^i),$$

$$\sigma_{e_{kj}}^* = \sigma_{e_{kj}} + \frac{1}{|Y_B|} (\sigma_{e_{k1}} A_{1j}^e + \sigma_{e_{k2}} A_{2j}^e + \sigma_{e_{k3}} A_{3j}^e),$$

$$\sigma_{d_{kj}}^* = \sigma_{d_{kj}} \frac{|Y_D|}{|Y_B|} + \frac{1}{|Y_B|} (\sigma_{d_{k1}} A_{1j}^d + \sigma_{d_{k2}} A_{2j}^d + \sigma_{d_{k3}} A_{3j}^d).$$

$A_{kj}^i, A_{kj}^e, A_{kj}^d$ - from the cell problems.

The cell problems

Solved **only once** - on the unit cell Y .

Intracellular:

$$\nabla \cdot (\sigma_i \nabla w_j^i) = 0, \text{ in } Y_B,$$

$$\sigma_i (\nabla w_j^i + e_j) \cdot n = 0, \text{ on } \Gamma,$$

w_j^i is Y periodic.

Extracellular:

$$\nabla \cdot (\sigma \nabla w_j) = 0, \text{ in } Y,$$

$$[\sigma \nabla w_j \cdot n] + (\sigma_e - \sigma_d) e_j \cdot n = 0, \text{ on } \Gamma,$$

w_j is Y periodic.

Finally,

$$A_{kj}^i = \int_{Y_B} \partial_k w_j^i, \quad A_{kj}^e = \int_{Y_B} \partial_k w_j, \quad A_{kj}^d = \int_{Y_D} \partial_k w_j.$$

3

The third chapter

Numerics

2D Numerical experiments, convergence.

- ▶ Geometry:
 - ▶ square domain, circular and elliptical inclusions
 - ▶ $\varepsilon \in \{1/5, 1/10, \dots, 1/40\}$
- ▶ Conductivities:
 $\sigma_{i11} = 1.741, \sigma_{i22} = 0.1934, \sigma_{e11} = 3.906, \sigma_{e22} = 1.970,$
 $\sigma_{d11} = \sigma_{d22} = 3.$
- ▶ Discretisation: $dt = 0.5$ and $dx \approx 0.3$

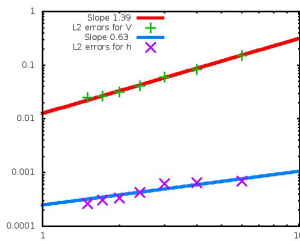
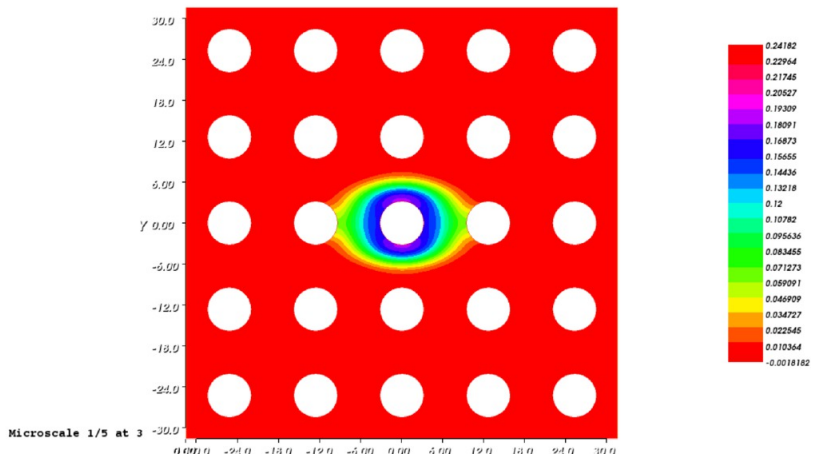


Figure: Convergence rate: 1.39 for V , 0.63 for h .

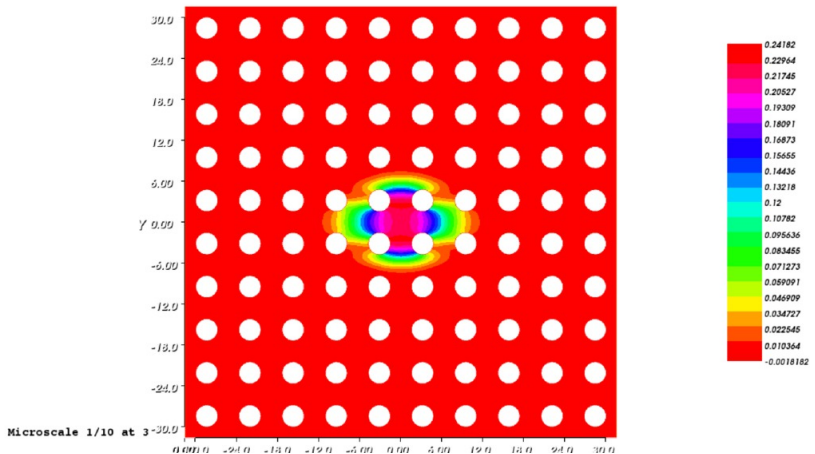
The numerical results

Homogenisation process - $\varepsilon = \frac{1}{5}$



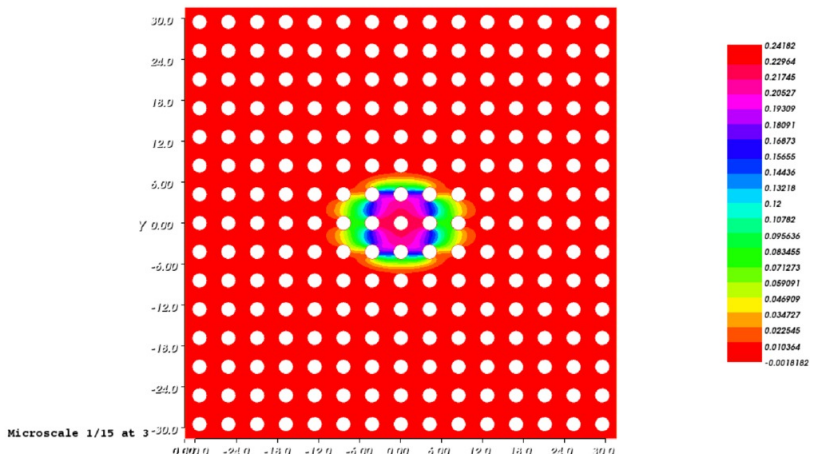
The numerical results

Homogenisation process - $\varepsilon = \frac{1}{10}$



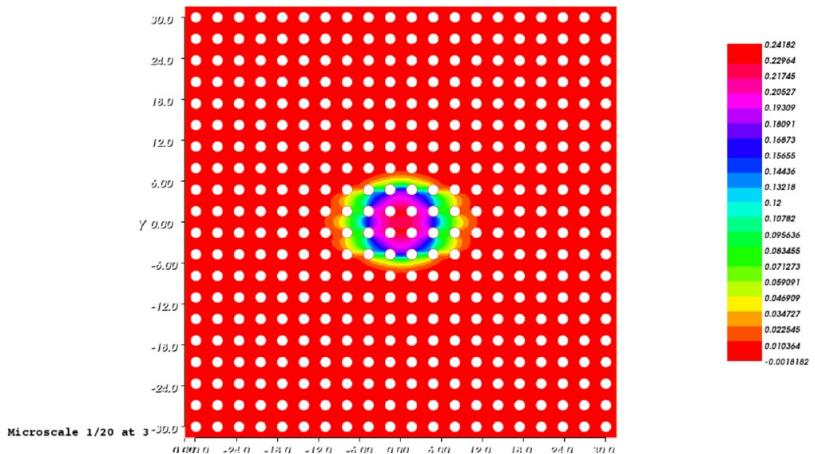
The numerical results

Homogenisation process - $\varepsilon = \frac{1}{15}$



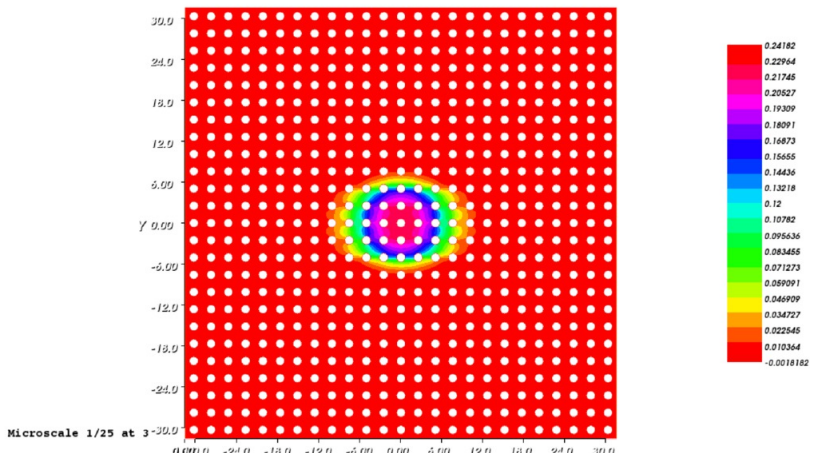
The numerical results

Homogenisation process - $\varepsilon = \frac{1}{20}$



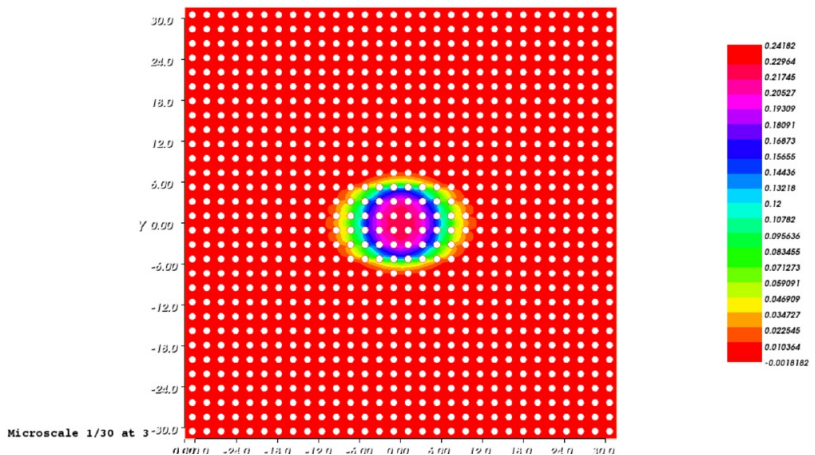
The numerical results

Homogenisation process - $\varepsilon = \frac{1}{25}$



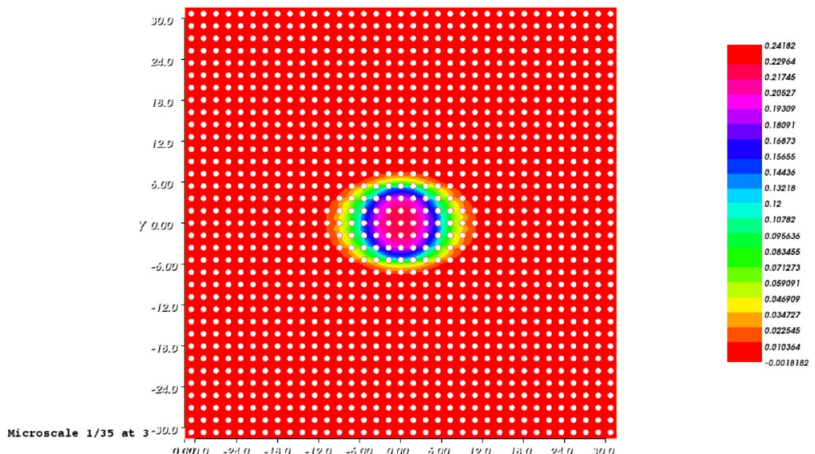
The numerical results

Homogenisation process - $\varepsilon = \frac{1}{30}$



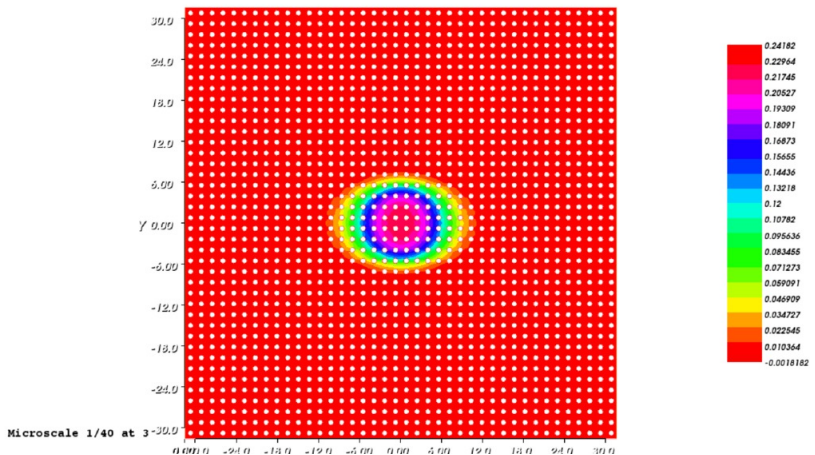
The numerical results

Homogenisation process - $\varepsilon = \frac{1}{35}$



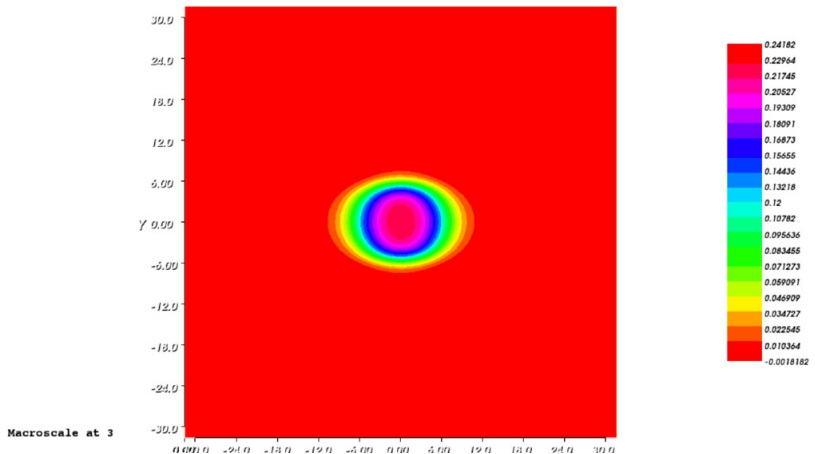
The numerical results

Homogenisation process - $\varepsilon = \frac{1}{40}$



The numerical results

Homogenisation process - $\varepsilon = \frac{1}{\infty}$



The numerical results, conductivities.

Geom	Vol fr	σ^d	$\sigma_{i_{11}}^*$	$\sigma_{i_{22}}^*$	$\sigma_{e_{11}}^*$	$\sigma_{e_{12}}^*$	$\sigma_{e_{21}}^*$	$\sigma_{e_{22}}^*$
-	-	-	1.74	0.19	3.9	0	0	1.97
circle	0.2	0.1	1.26	0.17	2.85	0.00	0.005	1.81
circle	0.2	1	1.26	0.17	2.99	0.01	0.005	2.02
circle	0.2	6	1.26	0.17	3.73	0.04	0.005	3.27
circle	0.2	3	1.26	0.17	3.29	0.02	0.005	2.53
circle	0.4	3	1.07	0.15	3.42	-0.17	0.02	3.53
circle	0.7	3	0.69	0.09	5.08	-2.09	-0.01	7.89
ellipse	0.2	3	1.13	0.18	2.82	0.06	0.00	2.58
ellipse	0.4	3	0.81	0.16	2.53	-0.03	-0.01	3.70
ellipse2	0.2	3	0.86	0.18	2.09	0.06	0.00	2.64

The numerical results, comparison.

Time $t = 0.5$

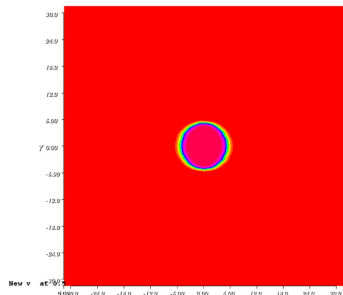
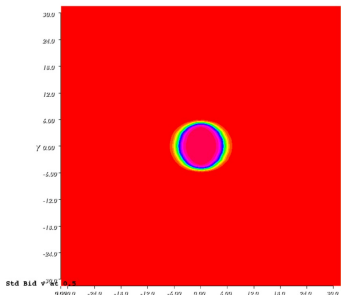


Figure: (Left) Standard bidomain. (Right) New model.

The numerical results, comparison.

Time $t = 1.0$

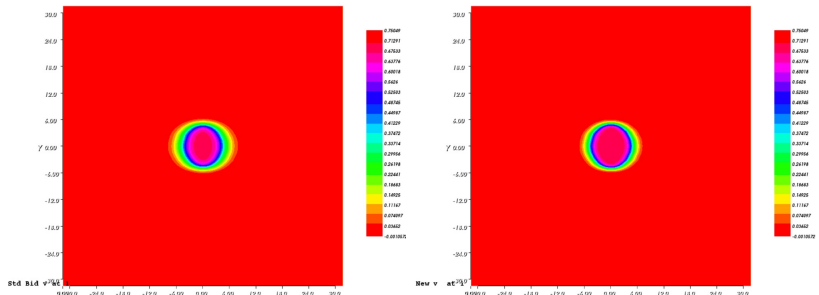


Figure: (Left) Standard bidomain. (Right) New model.

The numerical results, comparison.

Time $t = 1.5$

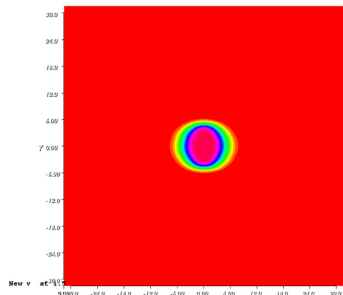
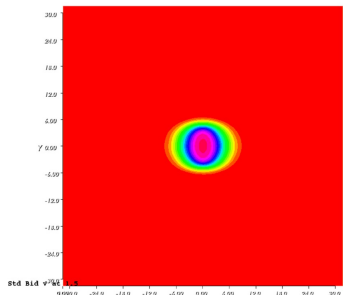


Figure: (Left) Standard bidomain. (Right) New model.

The numerical results, comparison.

Time $t = 2.0$

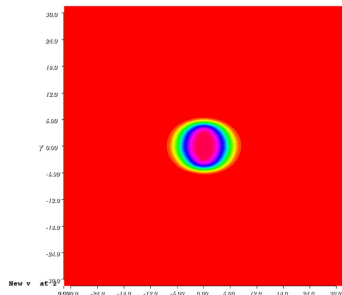
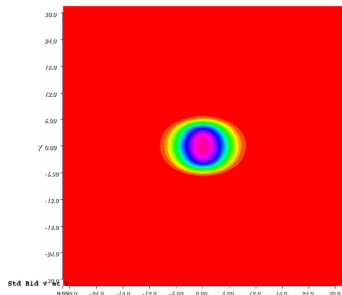


Figure: (Left) Standard bidomain. (Right) New model.

The numerical results, comparison.

Time $t = 2.5$

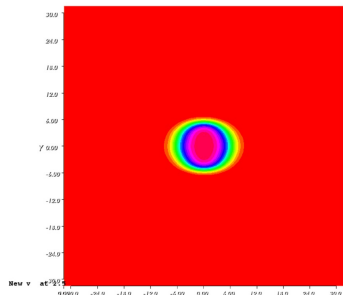
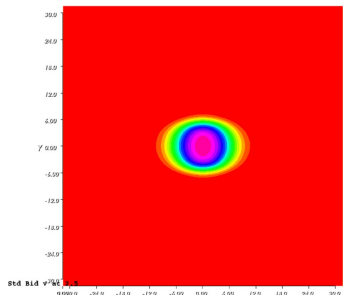


Figure: (Left) Standard bidomain. (Right) New model.

The numerical results, comparison.

Time $t = 3.0$

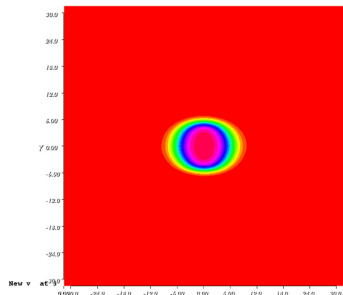
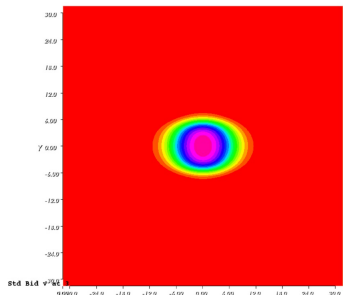


Figure: (Left) Standard bidomain. (Right) New model.

The numerical results, comparison.

Time $t = 3.5$

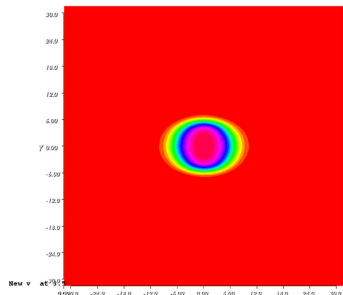
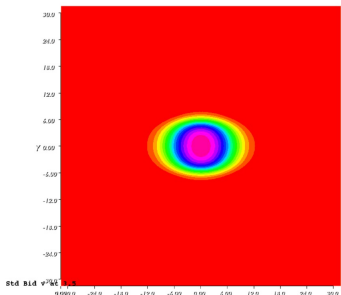


Figure: (Left) Standard bidomain. (Right) New model.

The numerical results, comparison.

Time $t = 4.0$

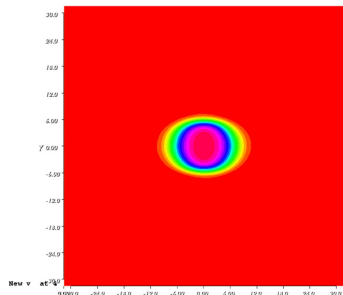
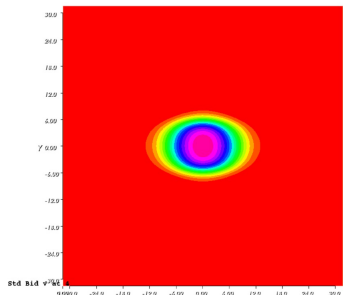
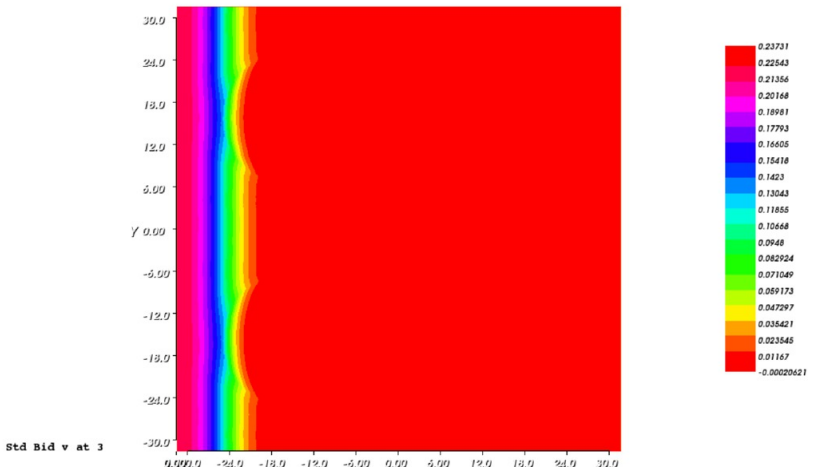


Figure: (Left) Standard bidomain. (Right) New model.

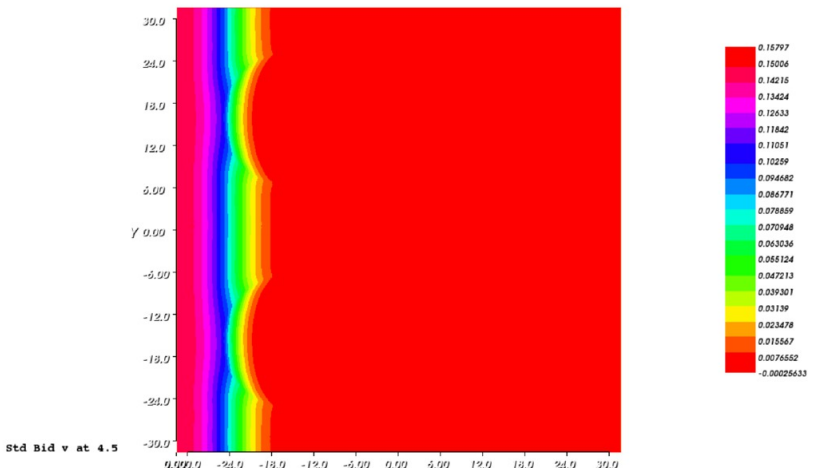
The numerical results, scars.

Time $t = 3.0$



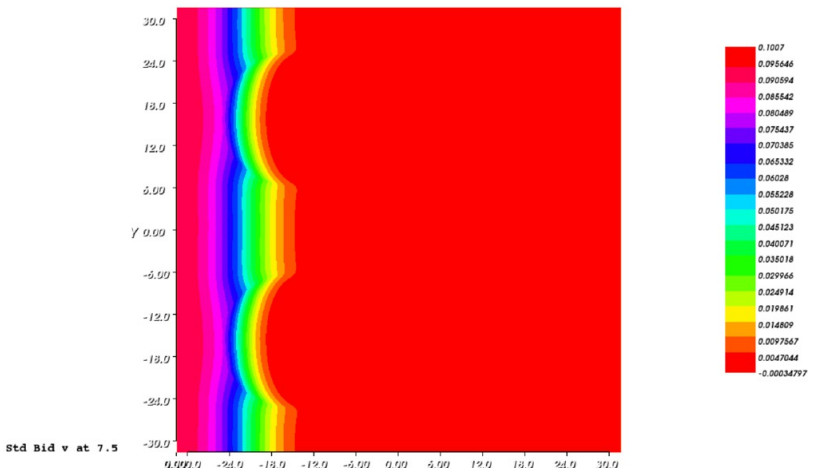
The numerical results, scars.

Time $t = 4.5$



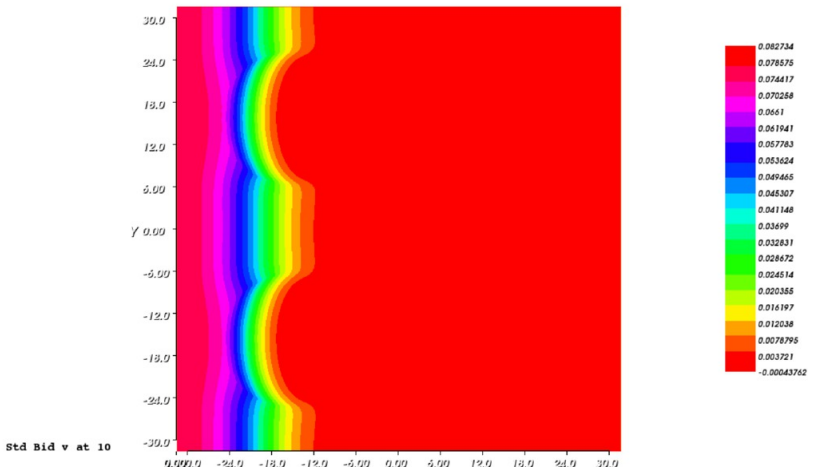
The numerical results, scars.

Time $t = 7.5$



The numerical results, scars.

Time $t = 10.0$



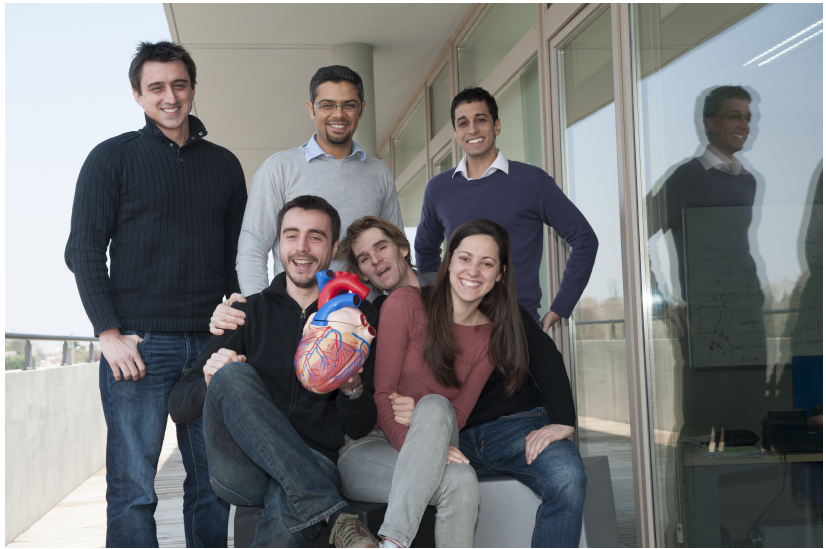
4

Conclusions

Discussion and further work

- ▶ New model \neq standard bidomain model
- ▶ Depends on
 - ▶ value of σ^d
 - ▶ volume fraction - larger inclusions bigger difference
 - ▶ geometry of inclusions
- ▶ Future work
 - ▶ Simulations for 3D model
 - ▶ The real geometries
 - ▶ The data reading - MRI? σ_d ?
 - ▶ The impact on the dynamics of spiral waves?
 - ▶ Can we trigger the re-entrant waves?

CARMEN team



Thank You.



Andjela Davidović
L'Aquila

September 7, 2014